
CdS(Se) and PbS(Se) Quantum Dots with High Room Temperature Quantum Efficiency in the Fluorine-Phosphate Glasses

Elena Kolobkova and Nikolay Nikonorov

Additional information is available at the end of the chapter

<http://dx.doi.org/10.5772/intechopen.68459>

Abstract

In this study, the luminescent properties of the CdS(Se) quantum dots (QDs) with the mean size of 2–4 nm, the (PbS)_n/(PbSe)_n molecular clusters (MCs) and PbS(Se) quantum dots (QDs) with the mean size of 2–5 nm embedded in the fluorine-phosphate glass are investigated. The dependence of the photo luminescence absolute quantum yield (PL AQY) on the sizes of the CdS(Se) QDs are studied. It is found that the PL AQY of the CdSe QDs increases monotonically to its maximum height and then falls down. The PL AQY of the CdS(Se) QDs can reach 50–65%. Luminescence of (PbS)_n/(PbSe)_n MCs embedded in fluorine-phosphate matrix and excited by UV radiation is obtained in the visible spectral region and its absolute quantum yield was up to 10%. The PbSe QDs have broadband photoluminescence with quantum efficiency about five times more than MCs (~50%) in the spectral range of 1–1.7 μm. Glasses doped with PbS(Se) QDs provide potential application as infrared fluorophores, which are both efficient and possess short life times. The glass matrix protects the QDs from external influence and their optical properties remain unchanged for a long time.

Keywords: quantum dots, molecular clusters, fluorine-phosphate glass, luminescence, absolute quantum yield

1. Introduction

1.1. Why fluorine-phosphate glasses?

Glass-crystalline materials (or glassceramics) are composite materials, usually consisting of a glassy matrix (glass phase) and nano-sized dielectric or semiconductor crystals or metallic

particles distributed in it. Glassceramics are formed by the growth of crystalline phase inside of a glass matrix. The growth of crystalline phase occurs as a result of the crystallization of amorphous phase during heat treatment. Glasses doped with CdS, CdSe, CdTe, PbS, PbSe nanocrystals are typical representatives of the nano-glassceramics or nanocomposite materials and usually used as a nonlinear optical media [1, 2]. Traditionally silicate glassy matrix has been used for QDs formation. These glasses are characterized by high synthesis temperature (1300–1500°C), long-time (tens of hours) and high temperature (500–700°C) of heat treatment [3–7].

In this study, we used a fluorine-phosphate (FP) glass featuring with a number of advantages compared to conventional silicate glasses, including low temperature synthesis and heat treatment, formation of quantum dots in the wide range of concentrations, short time of heat treatment and higher spatial distribution homogeneity. Two-stage heat treatment was afforded to get quantum dots (QDs) with narrow size distribution. The CdS and CdSe QDs dispersed in a fluorine-phosphate glasses are attracting much attention as nonlinear optical materials [1], but information about luminescent properties is not available.

In this communication, we present the results of our research designed for synthesis and characterization of yellow-red and IR emitting semiconductor quantum dots embedded in the fluorine-phosphate glass. The composites are fabricated by two-staged heat treatment and stabilization of synthesized II–VI and IV–VI semiconductor QDs into glass matrices. **Figure 1** demonstrates initial glasses and glasses after heat treatment.

1.2. Why phosphors for visible spectral region based on CdSe and CdS quantum dots?

QDs are a type of nanomaterials with good fluorescent properties. The size-dependent emission is probably the most attractive property of semiconductor nanocrystals. Among them, CdS and CdSe QDs are one of the most promising materials because QDs have bright luminescence in the visible range of the optical spectrum. For example, CdSe QDs have shown potential as superior biological labels [8–10], laser sources [11, 12] and tunnel diodes [13, 14].



Figure 1. Photo Initial glasses doped with CdS (1), CdSe (2), PbS (3) and PbSe (4) and glasses after heat treatment doped with CdSe QDs (with different sizes) (5) and PbSe (6).

Compared with conventional fluorescent dyes, CdS(Se) QDs have a wide continuously distributed excitation spectra, not only with symmetrical distributed narrow emission spectra, but also many other excellent properties such as adjustable color, excellent photochemical stability and high threshold of light bleaching [15].

However, colloidal synthesized bare quantum dots, including CdSe(S) QDs, usually have surface defects and cause to reduction in absolute photoluminescence (PL) quantum yield. The best PL absolute quantum yield (AQY) (quantum efficiency) reported for the as-prepared nanocrystals at room temperature is around 20% in the wavelength range of 520–600 nm and about a few percent or lower in the spectrum range above 600 nm. Also, in the spectrum range below 520 nm, it is a few percent or lower of total absolute quantum yield [13, 15]. In general, a low PL AQY is due to the surface states located in the bandgap of the nanocrystals. These surface states act as trapping states for the photogenerated charges. The origin of the surface trapping states is dangling bonds of the surface atoms [3, 16, 17]. Therefore, it is essential to control the QDs surfaces to reduce the surface defects by passivating the surface of QDs [18, 19].

The core/shell structures solve optical problems, such as low PL AQY and improve the stability of QDs. As was shown, the room temperature quantum efficiency of the band-edge luminescence of CdSe QDs could be improved to 40–60% by surface passivation with inorganic (ZnS) or organic (alkylamines) shells [18]. Due to the non-radiative processes, a reduction in the PL emission intensity was observed by annealing of the prepared samples in different environments (oxygen, hydrogen, and air).

Due to the failure of orange-red emitting materials in general, efforts were directed to synthesize colloidal CdS/CdSe QDs that can emit light with wavelengths that range from orange (600 nm) to red (650 nm). Nevertheless, both stability and reproducibility of the PL AQY are not predictable. With some inorganic and organic surface functionalization, the PL QY of synthesized colloidal CdSe nanocrystals is boosted more than 50% in the range of 520–650 nm. However, the emission efficiency for the orange-red color window is still low. Especially for red emission (around 650 nm), the PL QY of the nanocrystals in solution was nearly zero [15].

1.3. Why optical transparent glasses doped with CdS and CdSe quantum dots?

Semiconductor CdS and CdSe nanoparticles dispersed in a silicate glass matrix are attracting much attention [3–5]. The possibility of QDs formation in the optical glasses creates significant benefits for their application. Currently, optical transparent glasses doped with nanocrystals are of great interest for the modern element base of photonics. In these materials, the best properties of nanocrystals and glasses technology (possibilities of pressing and molding, sputtering, pulling optical fibers, using ion exchange technology) are easily combined. In addition, the glass matrix protects the QDs from external influence.

In the QDs doped silicate glasses, the PL spectra consist of two bands: a less intense high-energy band and a lower energy broader band. The first band occurs at a wavelength 10–20 nm higher than the absorption edge of QDs and is due to direct electron-hole recombination. This weak peak shifts to the higher wavelength with increasing particle size. The second band is due to surface defects and occurs at 800–900 nm spectral region. PL AQY is less than 30% for CdS(Se) QDs in the silicate glasses and decreases as the size of QD increases [4].

1.4. Optical composite materials with PbS and PbSe quantum dots as tunable near-IR phosphors

Semiconductor PbS and PbSe quantum dots have been widely investigated because of their unique optical and electronic properties. PbS and PbSe are a typical narrow bandgap ($E_g = 0.41$ eV, $E_g = 0.29$ eV) semiconductors with the Bohr's exciton radii 20 nm (for PbS) and 46 nm (for PbSe). Their large Bohr radius provides strong quantum confinement effect that can be easily realized in a wide range of QD size [20, 21].

Optical composite materials with PbS and PbSe QD are widely used in optical and photonic applications. For example, PbS(Se) QDs have potential applications in near-infrared photodetectors, photovoltaics and as saturable absorbers [22, 23]. In contrast to rare-earth ions-doped optical materials, lead chalcogenide quantum dot-doped glasses can provide tunable near-IR luminescence (about 1–2 μm) with high absolute quantum yield ($\geq 60\%$) by controlling the size and distribution of QDs [22–24]. Despite a lot of efforts spent to find a novel gain medium which can almost cover the whole optical communication window, it is essential to tailor the emission of QDs embedded in a glass matrix in a wide bandwidth of the optical communication network. Therefore, PbS and PbSe QDs are promising gain media for covering the whole optical communication window [24–28]. Several advances of controlled chemical synthesis of the materials have provided the ways to grow QDs and manipulate their size, shape and composition using different methodologies [29].

PbSe and PbS QDs with a band gap in the mid-infrared are interesting infrared phosphors materials. In the visible spectral range organic dyes usually present large PL AQY value than quantum dots, but infrared organic dyes have very low PL AQY suffer from poor photostability. On the other hand, the rare-earth ions can be used as the efficient infrared phosphors but they have small absorption cross sections and microsecond lifetimes. Infrared phosphors of PbS(Se), that are both efficient and possess short lifetimes, may find unique applications in the near-IR spectral range where biological tissues are relatively transparent, or as fluorescent materials in the fiber communication range of 1.3–1.5 microns.

Variation of temperature and duration heat treatment (HT) of the glasses doped with Pb, S or Se make possible to change sizes of PbS(Se) QDs in a wide range (2–15 nm). The choice of these parameters enhances the formation of nucleation centers (NCs) in the glass and leads to good size control and small size dispersions. The growth processes of lead chalcogenide QDs is based mainly on the phase decomposition from the over-saturated solid solution. Two-stage heat treatment of the glass afforded QDs with narrow size distribution.

Lead chalcogenide QDs have been synthesized in silicate glasses, fluorine-phosphate glasses and germanosilicate glasses [7, 30–32]. Among these glasses, fluorine-phosphate glasses have the largest solubility of lead chalcogenide compounds [32].

It is evident that during the process of formation and growth, these structures pass through the phase when their sizes are less than 1.0 nm and they do not possess semiconductor properties. This phase corresponds to the existence of lead chalcogenide compounds in a form of molecular clusters (MCs) [36]. The optical properties of MCs are considerably different from the properties of QDs.

In this study, we used a fluorine-phosphate glass (FPG) doped with high concentration of CdS, CdSe, PbSe and PbS QDs. FPGs are featured with a number of advantages compared to conventional silicate and borosilicate glasses. FPGs characterize low temperature synthesis, possibility for a wide range adjustment of the formed quantum dots concentration, low temperature and time of heat treatment and higher spatial distribution homogeneity of the QDs. We represent the luminescent properties of the fluorine-phosphate glasses doped with CdS, CdSe, PbSe and PbS QDs.

2. Preparation procedure

In order to investigate the effect of the QDs sizes on the PL properties, the fluorine-phosphate (FP) glasses $0.25\text{Na}_2\text{O}-0.5\text{P}_2\text{O}_5-0.05\text{ZnF}_2-0.1\text{Ga}_2\text{O}_3-0.05\text{AlF}_3-0.05\text{NaF}$ (mol%) doped with CdS, CdSe or PbSe (PbF_2+ZnS) and PbS (PbF_2+ZnSe) were synthesized. The glass synthesis was conducted in an electric furnace at 1050°C in the Ar-atmosphere using the closed glassy carbon crucibles. This method allows for maintaining the high concentrations of volatile components (such as Se, Se ore F) and avoiding the interaction with atmospheric air, thus preventing the fluorine-oxygen substitution reaction. After quenching, the glasses were annealed at 320°C for 1 h to release thermal stress and to form MCs. Then glasses were cut into pieces of 10×10 mm and were optically polished. Planar polished samples 0.4–1.0 mm thick were prepared for further investigation. Samples were heat treated using a muffle furnace (Nabertherm) with program temperature control to induce formation of CdS(Se) and PbS(Se) QDs at a temperature above glass transition temperature (T_g).

3. Luminescent properties of quantum dots in the fluorine-phosphate glasses

3.1. Fluorine-phosphate glasses doped with CdSe quantum dots

The emission properties of semiconductor nanocrystals can be evaluated by three key parameters, which are the brightness, the emission color and the stability of the emission.

Samples of the glass-containing CdSe QDs were prepared by heat treatment of $0.25\text{Na}_2\text{O}-0.5\text{P}_2\text{O}_5-0.05\text{ZnF}_2-0.1\text{Ga}_2\text{O}_3-0.02\text{PbF}_2-0.08\text{AlF}_3$ glass doped with 0.6 mol% CdSe. The glass transition temperature measured with STA 449 F1 Jupiter (Netzsch) differential scanning calorimeter (DSC) was found to be $400 \pm 3^\circ\text{C}$ (**Figure 2**). DSC curve of the glass doped with CdS and CdSe was identical. High crystallization peak in 430–460 temperature range confirms high concentration CdSe(CdS) QDs in the glass. Hence, on the base of DSC data, we have determined the regimes of heat treatment of the starting glasses which are necessary for the nanocrystalline phase production: temperature $T = 410^\circ\text{C}$, time 20–60 min.

The optical density spectra of the studied FP glass samples were recorded using a double-beam spectrophotometer Lambda 650 (Perkin Elmer) in the 1.5–5 eV spectral region with 0.1 nm resolution. Absorption spectra demonstrate that due to quantum size effect, the band gap of CdSe QDs increases from 2.2 to 3.0 eV, as the size of the nanocrystals decreases from 4.0 to 2.0 nm.

The emission color of the PL of the nanocrystals shifts continuously from red (centered at 730 nm) to orange (centered at 630 nm) as size of QDs decrease (**Figure 3**). QDs sizes were defined using data [34, 35].

In the PL spectra, the broad band with a large Stokes shift is dominant, and the band-edge PL is negligibly weak (**Figure 3**). The emission spectrum of samples is dominated by “deep trap” emission, strongly red shifted from the band edge (**Figures 3 and 4**). For registration of the emission spectra was used an EPP2000-UVN-SR (Stellar Net) fiber spectrometer. The luminescence was excited by semiconductor lasers ($\lambda = 405$ nm). **Figure 5** illustrates a luminescence shift from yellow to red with the increasing size of QDs.

Figure 6 demonstrates the excitation energy dependence of PL AQY magnitudes for glasses doped with CdSe QDs. The QDs concentration in the glasses 2 and 3 is equal (**Figure 3**), but AQY of the QD with size 3 nm is two times higher. The emission color of the PL of the QDs with size 3 nm is red with $\lambda_{\text{max}} = 700$ nm. Absolute quantum yield measurements were carried out inside the integrated sphere with Photonic Multichannel Analyzer (PMA-12, Hamamatsu) at room temperature. The measurement error for the absolute quantum yield was $\pm 1\%$.

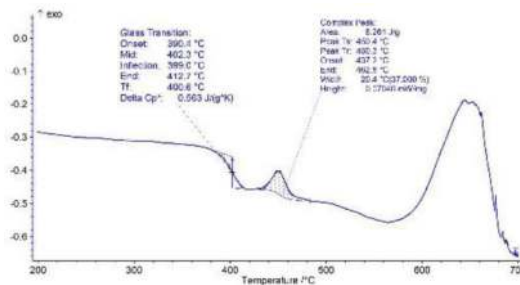


Figure 2. Thermal curve of the starting FP glass doped with Cd, Se and S measured with differential scanning calorimeter.

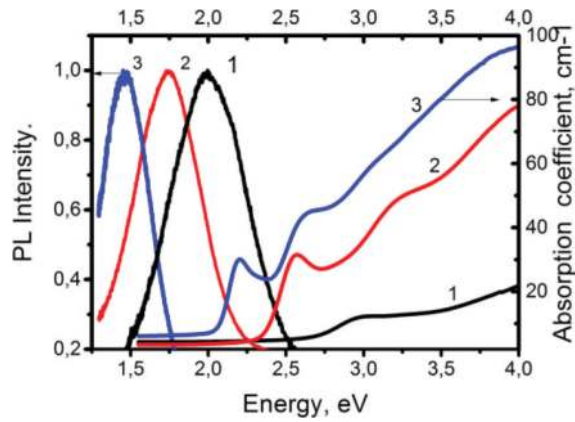


Figure 3. Absorption and luminescence spectra of the FP glass doped with CdSe QDs with sizes of 2.0 nm (1), 3.0 nm (2) and 4.0 nm (3). The excitation energy is 3.06 eV.

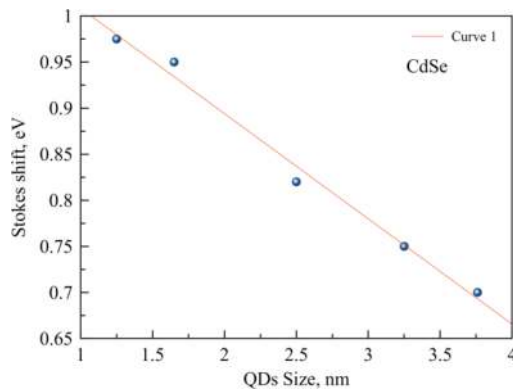


Figure 4. Dependence of the Stokes shift on the QDs size. Inset: Luminescence FP glasses doped with CdSe QDs with different sizes.

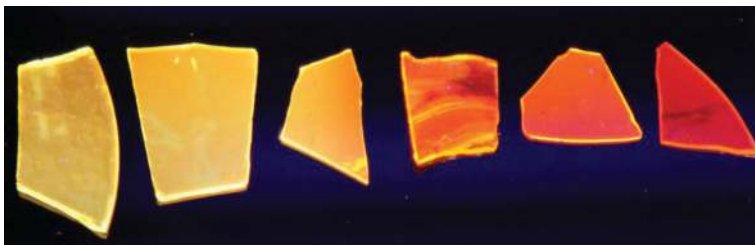


Figure 5. Photography of the luminescence of the glasses doped with CdSe QDs with sizes 2–4 nm.

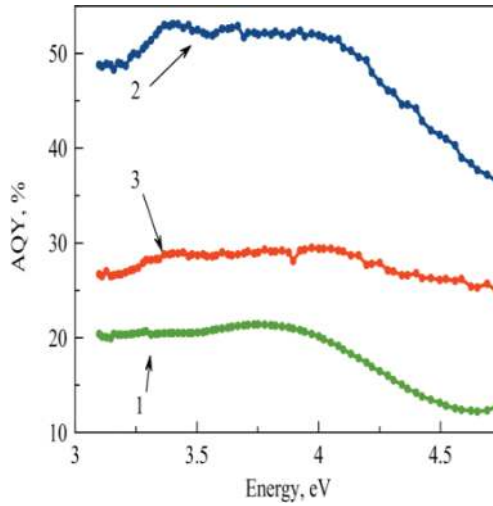


Figure 6. Dependence of the PL AQY for FP glasses doped with CdSe QDs with sizes 2.0 nm (1), 3.0 nm (2) and 4.0 nm (3) on the excitation energy.

The PL AQY magnitudes for glasses doped with CdSe QDs demonstrate a nonlinear dependence on the size (**Figure 7**). The PL AQY of the QDs increases monotonically from 4% to a maximum and then falls down to 30% (**Figure 4**). For convenience, the position with the maximum PL AQY is called the bright point as in Ref. [15]. The bright point for CdSe QDs in FP glass was observed for QDs with size 3.0 nm.

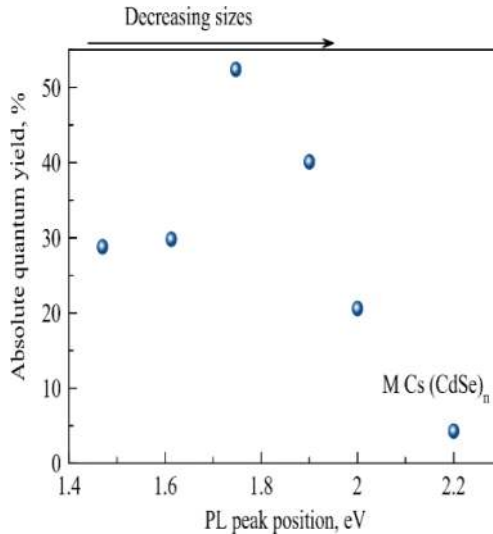


Figure 7. Dependence of the PL AQY on the PL peak position of the CdSe QDs.

The typical full width at half-maximum (FWHM) of the PL peak of the CdSe QDs ensemble at room temperature in FP glass, around 300–600 meV, is noticeably broader than that observed for colloidal QDs (30–70 meV) [15]. FWHM magnitudes decrease as QDs sizes increase (**Figure 8**).

3.2. Fluorine-phosphate glasses doped with CdS quantum dots

As a result of quantum confinement effects, the absorption bands of the colloidal semiconductors CdS QDs shift to the higher energy region compared with the band-gap energy of 2.5 eV in a CdS bulk crystal [15]. Heat treatment leads to this effect in the glasses. It was shown [36] that heat treatment has a significant impact on properties of glasses doped with CdS QDs. With increasing of the heat-treatment duration, the absorption band shifts to a lower energy side. These results indicate the formation and growth of the CdS QDs. Based on the theory of the quantum size effect in spherical QDs [37], the mean radii of prepared CdS QDs are estimated to be 2.3 and 3.5 nm. The observation of the clear absorption peaks indicates that the size-distribution width of the CdS QDs is rather small (**Figure 9**).

Figure 9 clearly shows effect of the heat treatment on the absorption and emission spectra of FP glasses doped with CdS QDs with sizes 2.3 and 3.5 nm. In PL spectra, the broad PL band with a large Stokes shift (1.2 eV) is dominant, and the band-edge PL is negligibly weak. The emission spectrum of samples is dominated by “deep trap” emission, strongly red shifted from the band edge.

Figure 9 demonstrates size dependence of the PL AQY magnitudes for glasses doped with CdS QDs with sizes 2.3, 3.5 and 1.5 nm.

The PL AQY magnitudes for glasses doped with CdS QDs with sizes 2.3–3.5 nm demonstrate weak dependence on the size (**Figure 10**). The PL AQY of the CdS QDs increases to 65% for QDs with size 2.3 nm and then slowly falls down to 60% for QDs with size 3.5 nm. In a whole range of the QDs sizes (1.8–3.5 nm) PL AQY magnitudes does not fall below 30%.

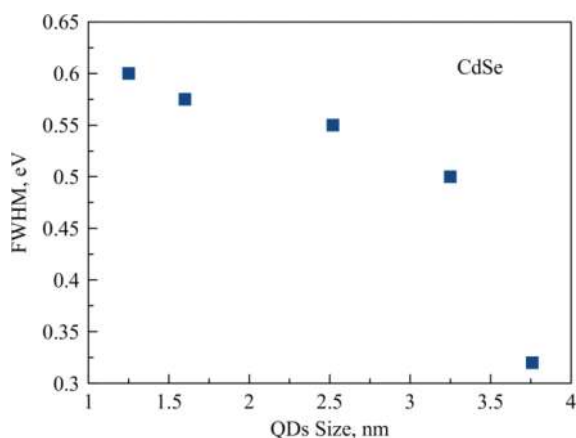


Figure 8. Dependence of the PL FWHM magnitudes for glasses doped with CdSe QDs with different sizes.

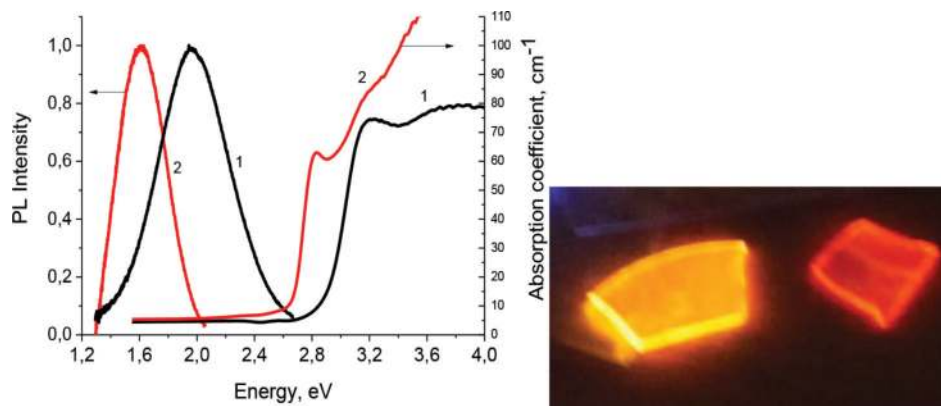


Figure 9. Absorption and luminescence spectra of the FP glasses doped with CdS QDs with sizes of 2.3 nm (1) and 3.5 nm (2). The excitation energy is 3.06 eV. Inset: Luminescence of the FP glasses doped with CdS QDs.

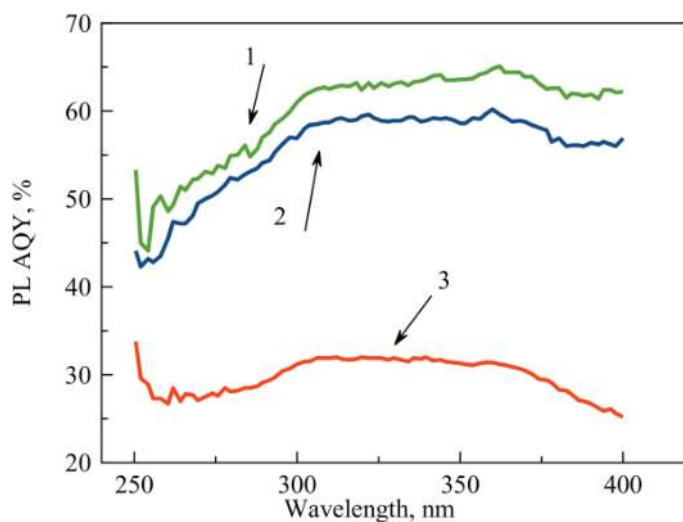


Figure 10. Dependence of PL AQY magnitudes for glasses doped with CdS QDs with sizes 2.3 nm (1), 3.5 nm (2) and 1.8 nm (3), respectively, on the excitation wavelength.

3.3. Stability of CdS and CdSe quantum dots in the fluorine-phosphate glasses

The PL properties of the CdS and CdSe nanocrystals prepared in the FP glasses, including the PL QY, the peak position and the PL FWHM, did not show any detectable change upon aging in air for several years.

It is known that under the various external factors (fluorescent lighting, laser and UV exposure in an oxygen environment) the CdS(Se) QDs sizes decrease [15] due to the formation of

the layer in which sulfur or selenium substitute for oxygen. This process is named photo-oxidation. Photo-oxidation destroys the luminescent centers and reduces PL AQY magnitudes of the colloidal QDs.

A stability of nanocrystals in the FPG were defined by an impulse wave laser photo-oxidation experiment at UV (355 nm), visible (532 nm) wavelengths and after interrelation with Hg lamp during 3 h.

Figure 11 shows the result of the experiment on the FP glass samples doped with CdSe QDs in a diameter of 4.5 nm. The laser power density was 15 mJ and durations of the interaction laser change was from 0 to 15 min.

Before and after irradiation, the absorption spectra of the four samples were identical. This result demonstrates that the photo-oxidation of the nanocrystals in the glass is negligible.

A related photo-oxidation experiment was done on CdSe and CdS nanocrystals. The optical densities of the three samples were within 10% of each other below 375 nm. The CdS sample showed an absorption peak at 418 nm and for the CdSe sample, it is at 420 and 450 nm. A 240 W Hg lamp illuminated the three samples simultaneously for 3 h at a large enough distance from the lamp to prevent significant heating. As above, the CdS and CdSe nanocrystals did not show the blue shifting of their absorption maximums and a general loss of optical density at all wavelengths of absorption. The magnitudes of quantum yields were within the error of measurement for all tested glasses before and after the UV radiation.

Our qualitative results demonstrate the enhanced photostability of the QDs synthesized in the FP glasses. We measured the absorption spectra and the quantum yields of FP glasses doped with QDs before and after irradiation during 12 months. No changes in absorption spectra and in quantum yield were detected. This combination of photostability and high quantum yield makes these materials very attractive for use in optoelectronic devices like LEDs.

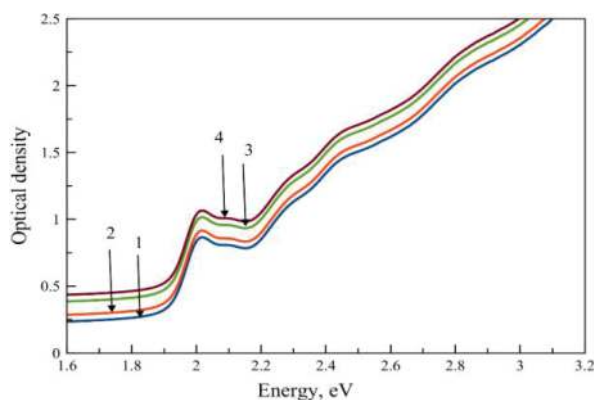


Figure 11. Absorption spectra of FP glasses doped with CdSe QDs with size of 4.5 nm after laser irradiation at power density 15 mJ during 0 min (1), 5 min (2), 10 min (3) and 15 min (4) at $\lambda_{exc} = 355$ nm. The diameter of the laser beam is 4 mm.

Absolute quantum yield allows to estimate the efficiency of converting UV light in the visible range and emphasizes the importance of this parameter for industrial applications of glasses doped with CdS(Se) QDs as luminescence down-shifting material or phosphor.

3.4. A fluorine-phosphate glass doped with CdS(Se) as a new type of red phosphor

The blue LED InGaN used as a basic component of the white LED emits with the spectra maximum at 450 nm. YAG:Ce³⁺ powder is a conventional phosphor with the spectral maximum at 570 nm and shifts the LED color temperature range toward the “warmer” white light. However, this composition gives the so-called “cold” white light, because their radiation does not cover the overall visible range. This “cold” white light is not always comfortable for eyes. Thus if one wants to get the composition of the emitters with “warm” white light, it is necessary to introduce an additional phosphor—some new component, introducing into the spectrum the red component with broad band luminescence and the maximum at 600–750 nm. Prospective for this task are, for instance, materials doped with manganese ions. However, this type of LEDs has a significant disadvantage—the absorption cross-section by manganese ions in the spectral range of 400–600 nm is negligible.

One can solve this problem with the use of other phosphor activators—CdS(Se) QDs with the maximum of the emission band at 650–700 nm, which introduces into the blue LED emission of the red component. As a result, the mixing of blue, green and red light takes place. In our work we have tried to solve the mentioned problems by means of the FP glasses doped with CdS(Se) QDs.

Figure 12 shows the CIE chromaticity coordinates of the FP(CdSe) glass heat treated at $T = 405^\circ\text{C}$ for 30 and 60 min and **Figure 13** illustrates CIE chromaticity coordinates of the FP(CdS) glass heat treated at $T = 415^\circ\text{C}$ for 10, 30 and 40 min. It is shown the increasing of the heat-treatment duration shifts the chromaticity coordinates from the yellow area ($x = 410$, $y = 370$) to the area of the diagram that corresponds to the red color ($x = 440$, $y = 380$).

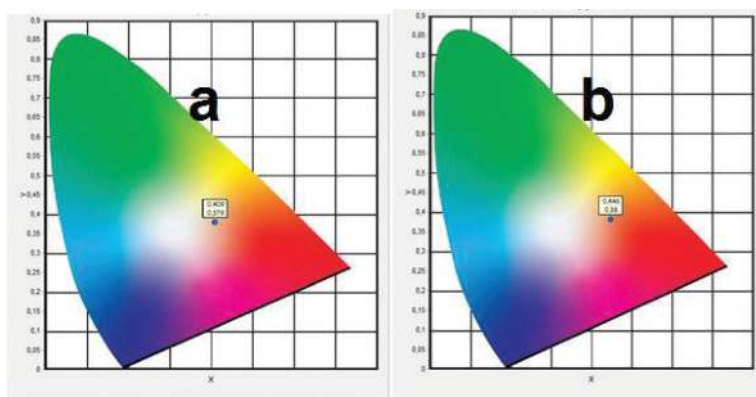


Figure 12. CIE chromaticity coordinates of the FP(CdSe) glass heat treated at $T = 405^\circ\text{C}$ during 30 min (a) and 60 min (b).

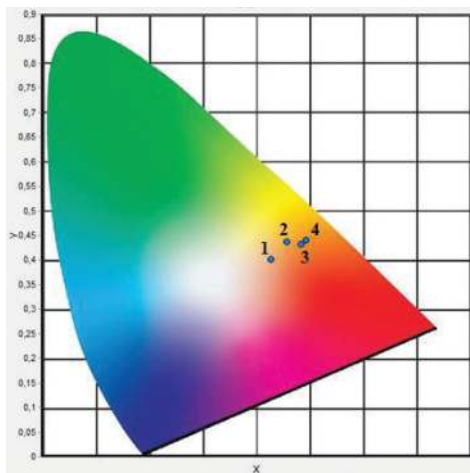


Figure 13. CIE chromaticity coordinates of the FP (CdS) glass heat treated at $T = 415^{\circ}\text{C}$ during 10 min (1), 30 min (2), 40 min (3) and 60 min (4).

In this study, a new type of red phosphor representing a fluorine-phosphate glass doped with CdS(Se) were synthesized using technology developed and applied earlier by Vaynberg [1]. These red phosphors with combination of green-yellow phosphors can be applied to fabricate the pc-WLEDs on the blue InGaN chips.

Absolute quantum yield allows estimating efficiency of converting UV light in the visible range that is why it is an important parameter for industrial applications of glasses doped with CdS(Se) QDs as luminescence down-shifting material or phosphor.

3.5. Fluorine-phosphate glasses doped with PbS and PbSe molecular clusters

Highly concentrated semiconductor components, which can be stored in glasses, is a main difference between FP glasses and previously studied silicate and borosilicate glasses. It is obviously expressed, that the concentration of MCs and QDs, which may be formed in the glass during heat treatment, is also significantly higher. High concentration and the uniform distribution of the activators should lead to high values of absolute quantum yield. DSC curves confirm the high concentration of the activator (**Figure 14**).

The glass transition temperature was found to be $400\text{--}408 \pm 3^{\circ}\text{C}$. Samples were heat treated to induce formation of PbS(Se) QDs at 410°C . Due to the high concentration of sulfur and selenium, crystallization peak induced by the precipitation of PbS(Se) QDs was observed.

As-prepared glasses doped with PbS(Se) demonstrate strong luminescence (when excited in UV spectral region) due to the MCs formation whereas the changes of the absorption coefficient are not large. The heat treatment at temperatures less than T_g results in the MCs' growth and increases the luminescence intensity [36–38]. For registration of the emission spectra excited at $\lambda = 405 \text{ nm}$ (3.06 eV), we used an EPP2000-UVN-SR (Stellar Net) fiber spectrometer.

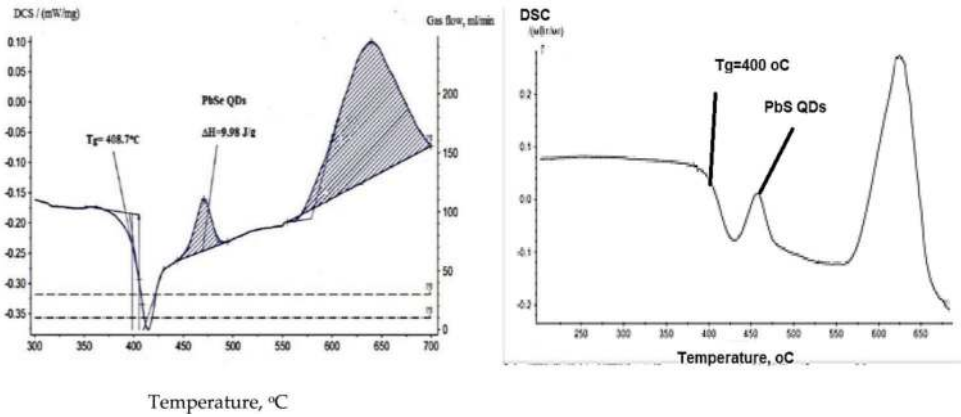


Figure 14. DSC curves of the initial glasses doped with PbSe (a) and PbS (b).

The optical density spectra of the studied FP glass samples were recorded using a double-beam spectrophotometer Lambda 650. (Perkin Elmer) in the 1.5–5 eV spectral region with 0.1 nm resolution and spectrophotometer Cary 500 (Varian) from 300 to 3000 nm (optical resolution was 0.5 nm).

PL excitation spectrum of the glass doped with MCs(PbS)_n can be observed in spectral range of 250–400 nm (Figure 15a). Asymmetric form of the PL excitation band by two ($\lambda_{\text{max}} = 290 \text{ nm}$ and $\lambda_{\text{max}} = 350 \text{ nm}$) indicates the existence of various sizes of the MCs. Figure 15b shows luminescence spectra of MCs(PbS)_n. The broad luminescence band of the MCs shifts from 570 to 700 nm due to the MCs sizes increasing. The absolute quantum yield of the as-prepared glasses doped with PbS (1) and after heat treatment (2) are shown in Figure 16a. The absolute

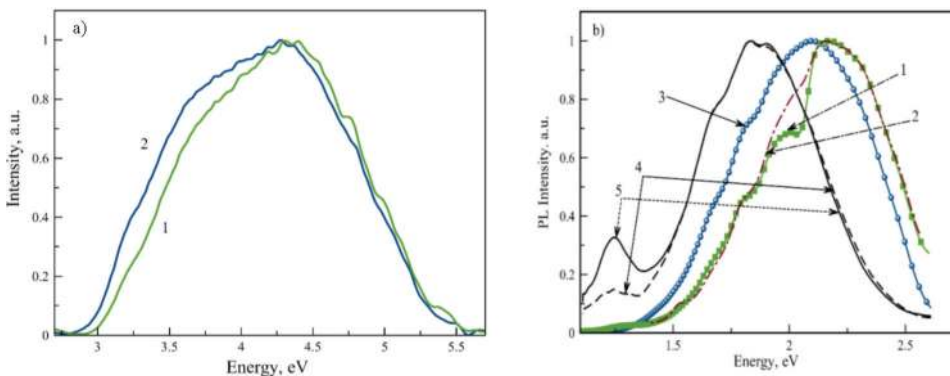


Figure 15. PL excitation spectrum of the glass doped with MCs (PbS)_n ($\lambda_{\text{lum}} = 540 \text{ nm}$) (a) Luminescence spectra of the glasses doped with MCs (PbS)_n: as-prepared (1) and after heat treatment at $T_{\text{HT}} = 410^\circ\text{C}$ within 10 min (2), 20 min (3), 30 min (4) and 40 min (5) ($\lambda_{\text{exc}} = 250 \text{ nm}$) (b).

quantum yield of the as-prepared glass doped with PbSe (1) and after heat treatment (2) shown in **Figure 16b**. **Figure 16c** shows the photography of the $(\text{PbS})_n$ MCs luminescence at $\lambda_{\text{exc}} = 365$ nm. Absolute quantum yield of the FP glass doped with PbS and PbSe MCs depends on excitation wavelength and changes from 10 to 2% (**Figure 16a** and **b**). The MCs are nucleation centers for the formation of PbS and PbSe QDs. It was shown [33, 36] that QDs formation in FP glasses leads to an increase in its intensity by a factor of five (**Figure 16a** and **b**).

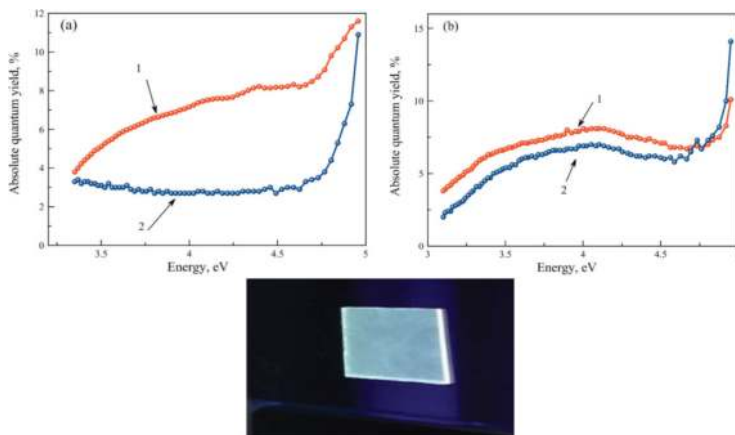


Figure 16. (a) Absolute quantum yield for the glasses doped with PbS as-prepared (1) and glass after heat treatment (2), (b) Absolute quantum yield for glass doped with PbSe as-prepared (1) and after heat treatment (2) and (c) photography of the $(\text{PbS})_n$ MCs luminescence at $\lambda_{\text{exc}} = 365$ nm.

The luminescence spectrum of FP (PbS) after heat treatment at $T = 360^\circ\text{C}$ within 90 min (1) (**Figure 17a**) demonstrates appearance of the second band (980 nm) due to small QDs formation. After heat treatment within 97 min (2) the luminescence band of the MCs was disappeared (**Figure 17a**).

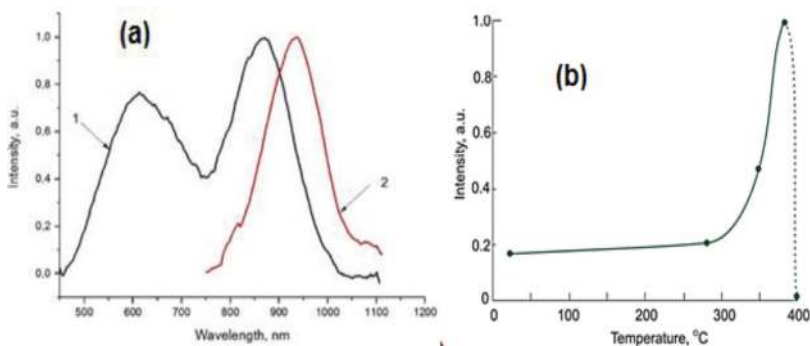


Figure 17. (a) Luminescence spectra of FP glass doped with MCs $(\text{PbS})_n$ after heat treatment at 400°C within 90 min (1) and 97 min (2), $E_{\text{exc}} = 3.06$ eV and (b) Luminescence intensity in maximum as a function of thermal treatment temperature.

Figure 18 shows the influence of heating on luminescence spectra. In this experiment, the sample preliminary thermal treated at 380°C was used. The increase of the sample temperature from 20 to 250°C led to seven times decrease of luminescence intensity and to the weak red shift of the luminescence band. This effect is reversible and can be repeated for many times [36]. The luminescence thermal quenching can be explained by a fact that with the temperature rise the electrons in the excited state can occupy high vibrational energy levels, which intersect the ground state level at configuration coordinate diagram. This allows the vibrational relaxation of the excited electrons to the ground state via phonon release without emission of radiation [36].

3.6. Fluorine-phosphate glasses doped with PbS and PbSe quantum dots

For luminescence measurement (scanning ranges 400–1100 nm and 900–1800 nm) with fixed excitation wavelength ($\lambda_{\text{ex}} = 808$ nm) Stellar Net EPP2000-UVN-SR fiber spectrometer was used (optical resolution 0.5 nm). A semiconductor laser with pumping power 0.1 W excited the luminescence.

When heat-treatment duration or temperature increase, the new band appears with $\lambda_{\text{max}} = 1000$ nm. It is due to the PbSe (S) QD formation with the sizes below 2.0 nm (**Figure 16a**). Increase of the heating temperature and time results in a prominent change of the absorption spectra and appearance of discrete spectra corresponding to QDs.

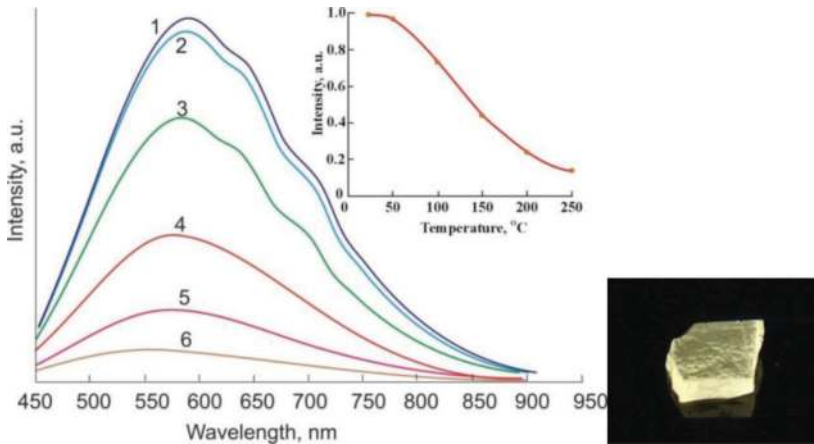


Figure 18. The influence of the temperature of the FP glasses doped with $(\text{PbSe})_n$ MCs on the luminescence intensity. The luminescence spectra were measured at temperature of (1) 22°C, (2) 50°C, (3) 100°C, (4) 150°C, (5) 200°C and (6) 250°C. Excitation wavelength was of 405 nm. Inset: Luminescence intensity in maximum via the temperature of the sample and photo of the luminescence of the FP glass doped with $(\text{PbSe})_n$ MCs.

To precipitate PbS QDs, glass samples were heat treated at temperature 410°C within 20–90 min (**Figure 19**). Based on hyperbolic band model obtained from $k \times p$ calculations [21], average diameters of these PbS QDs were found to be 3.0, 3.9 and 4.9 nm. QDs sizes were calculated using formula:

$$E_0 = 0.41 + \frac{1}{0.0252 \cdot D^2 + 0.283 \cdot D} \quad (1)$$

where E_0 —energy gap of PbS QDs (eV) and D —diameter of QDs in nm.

Increasing heat-treatment time and temperature leads to shifting of luminescence bands of the PbS QDs to 970, 1300 and 1500 nm (**Figure 19**) and absorption bands (to 920, 1100 and 1400 nm). Stokes shift changes from 80 to 50 meV due to the changing of QDs sizes from 3.0 to 4.9 nm (**Figure 21b**).

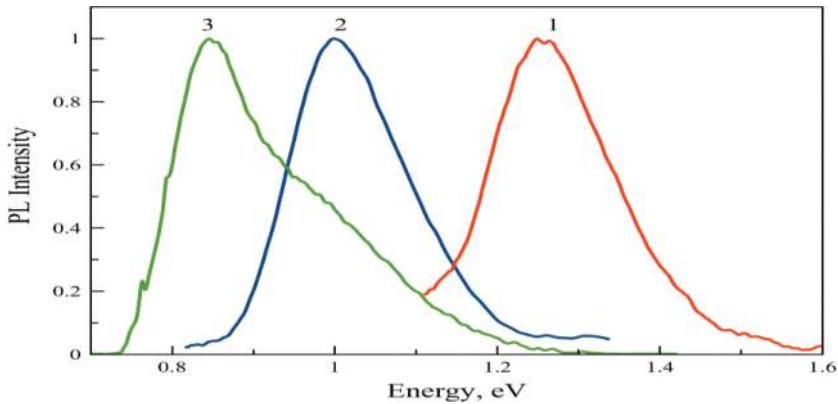


Figure 19. Luminescence spectra of the glasses doped with PbS QDs with sizes 3 nm (1), 3.9 nm (2), 4.9 nm (3) and $\lambda_{exc} = 808$ nm.

Figure 20 shows absorption and luminescence spectra of PbSe QDs formed in glasses. Increasing of the heating time results in prominent changes of absorption spectra of the FP glass doped with PbSe and leads to appearance of discrete spectra corresponding to QDs. Based on hyperbolic band model obtained from tight binding calculation using experimental energy values E_g , we can estimate the PbSe QD sizes [39] according to Eq. (2),

$$E_g(D) = E_g(\infty) + \frac{1}{0.0105 \cdot D^2 + 0.2655 \cdot D + 0.0667} \quad (2)$$

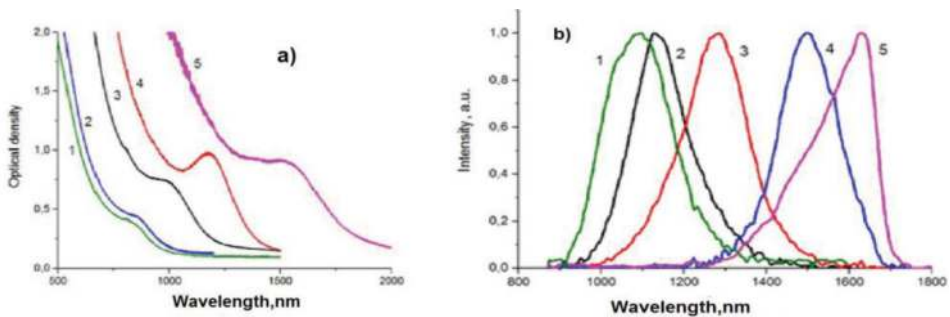


Figure 20. Absorption (a) and luminescence (b) spectra of the glasses doped with PbSe QDs with sizes 2.5 nm (1), 3.0 nm (2), 3.7 nm (4), 5.1 nm (5), $\lambda_{exc} = 808$ nm.

where D is the effective diameter of the quantum dots (nm), E_g is the energy gap of PbSe quantum dots (eV) and $E_g(\infty)$ is the energy bandgap of bulk PbSe semiconductor (0.29 eV).

When heat-treatment time and temperature are increased, absorption peaks shifts to 870–1540 nm and luminescence bands shifts to 1050–1650 nm. Stokes shift of QDs changes from 335 to 60 meV when size varies from 2.5 to 5.1 nm (**Figure 21a**).

It can be deduced that heat-treatment conditions define the formation characteristic of PbS (Se) QDs in glass (such as the beginning growth temperature, growth rate, density in glass matrix, size and size distribution of QDs, etc.).

Because of matching of the PL characteristic with window (1330 nm) of PbSe QD-embedded glass (see the **Figure 4**, curve 3), we choose this glass as the representative sample to characterize the optical amplification at the 1330 nm window. Signals at 1330 nm with different

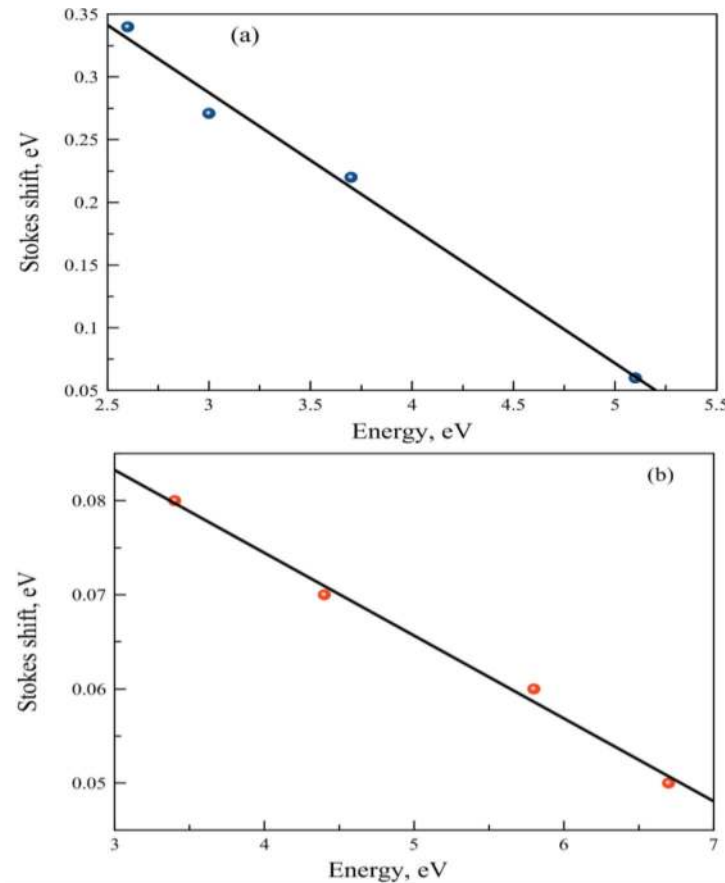


Figure 21. Stokes shift versus QDs diameter for PbS (a) and PbSe (b) QDs.

pump power values were measured. It can be found that the intensity enhances gradually with increasing of power. Even when the pump power reaches from 500 to 1000 mW, no obvious signal saturation is detected. This allows that FP (PbS and PbSe) glasses can be potentially applied in broadband amplifiers and confirm the high photo-stability of the QDs synthesized in the FP glasses. We also measured the absorption spectra and quantum yields of FP glasses doped with QDs before and after irradiation during 12 months. No changes in absorption spectra and in quantum yield were detected.

The FP glasses doped with PbSe and PbS QDs are infrared fluorophores, which are efficient, photo-stable and possess short lifetimes. These materials may find unique applications for fluorescent imaging.

4. Conclusions

The CdS and CdSe nanocrystals synthesized in the fluorine-phosphate glass represents a series of excellent emitters in the orange-red spectral region (600–750 nm) in terms of their PL AQY and the FWHM of the PL spectra, and they show the photo- and chemical stability of the emission for a long time.

The photoluminescence quantum yield of CdSe QDs rises monotonically to a maximum value and then decreases gradually with the size increase of QDs. Such a maximum (a PL “bright point”) is in 650–750 nm spectral range.

The PL AQY magnitudes for glasses doped with CdS QDs with sizes of 2.3–3.5 nm demonstrate weak dependence on the size and reaches 65%.

We suggest that origin of these dependences is the difference in the interaction mechanisms between CdSe and CdS quantum dots and glass network.

Experimental results suggest that the existence of the PL bright point is a general phenomenon of CdSe QDs and similarly is a signature of an optimal surface structure reconstruction of the nanocrystals grown in a liquid or in a glass. Absolute quantum yield magnitude of luminescence glasses doped with CdS (Se) QDs can reach 50–65%, which is two times higher than it was reported earlier in silicate glasses. It opens up new prospects for using such materials as phosphors for white LEDs and down-convertors for solar cells.

It was shown that heat treatment of the FP glasses leads to formation of (PbS)_n and (PbSe)_n molecular clusters, which exhibit luminescent properties in visible range with quantum efficiency from 2 to 10%. Increasing the heat-treatment temperature results in the PbS and PbSe QDs (sizes of 3–5 nm) formation with high concentration (~1 mol%). The QDs have broadband photoluminescence with quantum efficiency about five times more than MCs (~50%) in the spectral range of 1–1.7 μm. FP glasses doped with PbSe and PbS QDs are infrared fluorophores, which are both efficient and possess short lifetimes. These materials may find unique applications for fluorescent imaging tagging in the near-IR spectral range or as fluorescent materials in the fiber communication range of 1.3–1.5 microns.

Acknowledgements

Research was funded by Russian Science Foundation (Agreement #14-23-00136).

Author details

Elena Kolobkova^{1,2*} and Nikolay Nikonorov¹

*Address all correspondence to: kolobok106@rambler.ru

1 Department of Optical Informatics Technologies and Materials, ITMO University, Saint-Petersburg, Russia

2 St. Petersburg State Institute of Technology (Technical University), St. Petersburg, Russia

References

- [1] Vaynberg B, et al. High optical nonlinearity of $\text{CdS}_x\text{Se}_{1-x}$ microcrystals in fluorine-phosphate glass. *Optics communications*. 1996;**132**(3-4):307-310
- [2] Guerreiro PT, Ten S, Borrelli NF, Butty J, Jabbour GE, Peyghambarian N. PbS quantum-dot doped glasses as saturable absorbers for mode locking of a Cr: forsterite laser. *Applied Physics Letters*. 1997;**71**:1595-1597
- [3] Heo J, Liu C. PbS quantum-dots in glass matrix for universal fiber-optic amplifier. *Journal of Materials Science: Materials in Electronics*. 2007;**18**:S135-S139
- [4] Borrelli NF, et al. Quantum confinement effects of semiconducting microcrystallites in glass. *Journal of Applied Physics*. 1987;**61**:5399-5409
- [5] Su Z, et al. Selenium molecules and their possible role in deep emission from glasses doped with selenide nanocrystals. *Journal of Applied Physics*. 1996;**80**:1054-1055
- [6] Xu KM, et al. Optical properties of CdSe quantum dots in silicate glasses. *Journal of Non-Crystalline Solids*. 2010;**356**:2299-2301
- [7] Loiko PA, Rachkovskaya GE, Zaharevich GD, Gurin VS, Gaponenko MC, Yumashev KV. Optical properties of novel PbS and PbSe quantum dot-doped alumino-alkali-silicate glasses, *Journal of Non-Crystalline Solids*. 2012;**358**:1840-1845
- [8] Han M, et al. Quantum-dot-tagged microbeads for multiplexed optical coding of biomolecules. *Nature Biotechnology*. 2001;**19**:631-635
- [9] Bruchez M, et al. Semiconductor nanocrystals as fluorescent biological labels. *Science*. 1998;**281**:2013-2016

- [10] Chan WCW, Nie SM. Quantum dot bioconjugates for ultrasensitive nonisotopic detection. *Science*. 1998;**281**:2016-2018
- [11] Artemyev M, et al. Light trapped in a photonic dot: Microspheres act as a cavity for quantum dot emission. *Nano Letters*. 2001;**1**:309-314
- [12] Klimov VI, et al. Optical gain and stimulated emission in nanocrystal. *Science*. 2000;**290**: 314-317
- [13] Sundar VC, et al. Full color emission from II-VI semiconductor quantum dot-polymer composites. *Advance Materials*. 2000;**12**:1311-1312; Novel light emitting devices using cadmium selenide nanocrystals. Abstracts of papers of the American chemical society. 220. pp. U206-U206.
- [14] Schlamp MC, Peng X, Alivisatos AP. Improved efficiencies in light emitting diodes made with CdSe(CdS) core/shell type nanocrystals and a semiconducting polymer. *Journal of Applied Physics*. 1997;**82**:5837-5842
- [15] Qu L, Peng X. Control of photoluminescence properties of CdSe nanocrystals in growth. *Journal of American Chemical Society*. 2002;**124**(9):249-255
- [16] Fu H, Zunger A. InP quantum dots: Electronic structure, surface effects, and the red-shifted emission. *Physical Review B: Condensed Matter and Materials Physics*. 1997;**56**: 1496-1508
- [17] Talapin DV, et al. Highly luminescent monodisperse CdSe and CdSe/ZnS nanocrystals synthesized in a hexadecylamine-trioctylphosphine oxide-trioctylphosphine mixture. *Nano Letters*. 2001;**14**:207-211
- [18] Wang X, et al. Surface-related Emission in highly luminescent CdSe quantum dots. *Nano Letters*. 2003;**3**(8):1103-1106
- [19] Kim JM, et al. Photoluminescence enhancement in CdS quantum dots by thermal annealing. *Nanoscale Research Letters*. 2012;**7**:482-489
- [20] Kang FW. Wise, Electronic structure and optical properties of PbS and PbSe quantum dots. *The Journal of the Optical Society of America B*. 1997;**14**:1632-1646
- [21] Wisem FW. Lead salt quantum dots: The limit of strong quantum confinement. *Accounts of Chemical Research*. 2000;**33**:773-780
- [22] Sargent EH. Infrared quantum dots. *Advanced Materials*. 2005;**17**:515-522
- [23] Akiyama T, Kuwatsuka H, Simoyama T, Nakata Y, Mukai K, Sugawara M, Wada O, Ishikawa H. Nonlinear gain dynamics in quantum-dot optical amplifiers and its application to optical communication devices. *The IEEE Journal of Quantum Electronics*. 2001;**37**:1059-1065
- [24] Schaller RD, Petruska MA, Klimov VI. Tunable near-infrared optical gain and amplified Spontaneous emission using PbSe nanocrystals. *The Journal of Physical Chemistry B*. 2003;**107**:13765-13768

- [25] Pang F, Sun X, Guo H, Yan J, Wang J, Zeng X, Chen Z, Wang T. A PbS quantum dots fiber amplifier excited by evanescent wave. *Optics Express*. 2010;**18**:14024-14030
- [26] Dong G, Wu G, Fan S, Zhang F, Zhang Y, Wu B, Ma Z, Peng M, Qiu J. Formation, near-infrared luminescence and multi-wavelength optical amplification of PbS quantum dot-embedded silicate glasses. *Journal of Non-Crystalline Solids*. 2014;**383**:192-195
- [27] Moreals I, Lambert K, Smeets D, Muynck DD, Nollet T, Martins JC, Vanhaecke F, Vantomme A, Delerue C, Allan G, Hens Z. Size-dependent optical properties of colloidal PbS quantum dots. *ACS Nano*. 2009;**3**:3023-3030
- [28] Kolobkova EV, Lipovskii AA, Petrikov VD. Fluorophosphate glasses containing PbSe quantum dots. *Glass Physics and Chemistry*. 2002;**28**:246-250
- [29] Lipovskii AA, et al. Formation and growth of semiconductor nanocrystals in phosphate glass matrix. *Journal of the European ceramic society*. 1999;**19**(6-7):865-869
- [30] Dantas NO, Silva RS, Qu F. Optical properties of PbSe and PbS quantum dots embedded in oxide glass. *Physica Status Solidi B*. 2002;**232**:177-181
- [31] Kolobkova EV, Lipovskii AA, Petrikov VD, Melekhin VG. Fluorophosphate glasses with quantum dots based on lead sulfide. *Glass Physics and Chemistry*. 2002;**28**:251-255
- [32] Martin JL, Rivera R, Cruz SA. Confinement of excitons in spherical quantum dots. *Journal of Physics: Condensed Matter*. 1998;**10**:1349-1361
- [33] Lipatova ZO, Kolobkova EV, Aseev VA. Kinetics and luminescence of cadmium sulfide quantum dots in fluorine-phosphate glasses. *Optics and Spectroscopy*. 2015;**119**(12):229-233
- [34] Norris D, Bawendi MG. Measurement and assignment of the size-dependent optical spectrum in CdSe quantum dots. *Physical Review B*. 1996;**53**(24):16338-16446
- [35] Norris DJ, Bawendi MG. Structure in the lowest absorption feature of CdSe quantum dots. *The Journal of Chemical Physics*. 1995;**103**(130):5260-5268
- [36] Kolobkova EV, Kukushkin DS, Nikonorov NV, Shakhverdov TA, Sidorov AI, Vasiliev VN. Luminescent properties of fluorophosphate glasses with lead chalcogenides molecular clusters. *Journal of Luminescence*. 2015;**162**:36-40
- [37] Moller K, Bein T, Herron N et al. Encapsulation of lead sulfide molecular clusters into solid matrices: Structural-analysis with x-ray absorption-spectroscopy. *Inorganic chemistry*. 1989;**28**:2914-2919.
- [38] Evans CM, Guo L, Peterson JJ, Maccagnano-Zacher S, Krauss TD. Ultrabright PbSe magic-sized clusters. *Nano Letters*. 2008;**8**:2896-2899
- [39] Allan G, Delerue C. Confinement effects in PbSe quantum wells and nanocrystals, *Physical Review B*. 2004;**70**:245321